

# Optimized Design of Double Diaphragm Based MEMS Pressure Sensor for Wider Range and Better Sensitivity

Suja K. J., Vidya Gopal T. V., Rama Komaragiri

**Abstract**— Microelectromechanical system based silicon pressure sensors have undergone a significant growth in the last few years. The sensitivity, maximum measurable pressure and linear range of pressure sensors highly depend upon the diaphragm structure. In this work, single and double diaphragm based pressure sensors are designed and simulated and these can be used for high pressure measurements. A novel method of sensitivity enhancement by optimizing the thickness of double diaphragms is presented in this work. Also a study of the bulk micromachined silicon piezoresistive pressure sensor and surface micromachined stacked diaphragm pressure sensor are presented, simulated and compared with respect to deflection and sensitivity. Microelectromechanical system pressure sensors have been simulated with different diaphragm structures for obtaining wider operation range with better sensitivity. The performance of silicon and silicon on insulator pressure sensors at a given pressure are compared. The doping concentration of the piezoresistor is varied from  $10^{15} \text{ cm}^{-3}$  to  $10^{20} \text{ cm}^{-3}$  and the sensitivity of pressure sensors are compared. Evaluating different structures of pressure sensors and optimizing doping concentrations as  $10^{17} \text{ cm}^{-3}$ , the double SOI sensor shows better pressure sensitivity.

**Keywords**— MEMS, Piezoresistive Pressure Sensor, Surface micromachining, Bulk micro machining, Sensitivity

## I. INTRODUCTION

Micro Electro Mechanical System (MEMS) devices are generally considered as micro scale system consisting of micro dimensional mechanical sensors, actuators and microelectronic circuits. The objective of this work is to model and evaluate the performance of MEMS piezoresistive pressure sensor under the performance parameters like deflection and sensitivity of the diaphragm. MEMS based pressure sensors are mainly characterized into piezoresistive and capacitive type according to the electrical sensing mechanism [1].

The pressure sensor works on the principle that change in piezoresistivity occurs due to an applied pressure on the diaphragm, the fundamental concept of piezoresistive effect. Most of them use silicon for diaphragm and piezoresistive property of silicon or polycrystalline silicon as sensing mechanism [2-7]. In piezoresistive pressure sensor the die is made up of silicon substrate with a cavity which is produced by etching from one side of the substrate.

**Manuscript received November 15, 2013.**

**Suja K J**, Electronics and Communication Engineering Department , NIT Calicut, Kerala, India.

**Rama Komaragiri**, Electronics and Communication Engineering Department , NIT Calicut, Kerala, India.,

**Vidya Gopal T V**, Electronics Department, Mar Athanasius College of Engineering , Kothamangalam ,Kerala, India.

The portion above the cavity is the diaphragm, which deflects when pressure is applied on the back face of the diaphragm. The diaphragm can be square, rectangular or circular in shape [8]. Four piezoresistors ( $R_1$ - $R_4$ ) are placed at maximum stress locations on the diaphragms as shown in Fig.1. These four piezoresistors are connected in a wheat stone bridge configuration. As a result of induced stress, the resistance change and the bridge is out of balance which results in a output voltage. If  $V_{in}$  is the input voltage to bridge, the output voltage  $V_{out}$  which is proportional to the applied pressure is given by eqn (1).

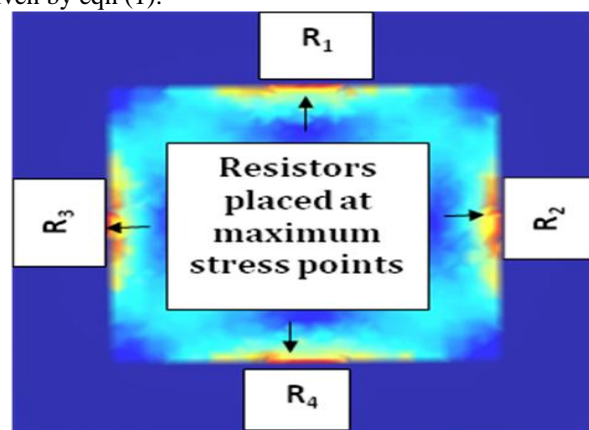


Fig.1 Placement of resistors on the square diaphragm

$$V_{out} = \left( \frac{R_3}{R_1 + R_3} - \frac{R_4}{R_2 + R_4} \right) V_{in} \quad (1)$$

When a pressure is applied, the diffused piezoresistors on the top silicon layer senses the induced stress. The performance of the piezoresistive pressure sensor depends on the dimensions of the diaphragm and the position of the resistors on the diaphragm [9]. Therefore a large diversity in the output characteristics can be observed for different dimensions of the diaphragm and different arrangement of resistors on the diaphragm. Sensitivity of the pressure sensor highly depends on the pressure range, size, shape and thickness of the diaphragm. Diaphragm dimensions are determined by sensor sensitivity and burst pressure (maximum nondestructive pressure) .The sensitivity of pressure sensor can be increased by decreasing the diaphragm thickness but there is a certain limit and over that limit undesired nonlinear effects occur when one uses the pressure sensor. A study of the bulk micromachined silicon piezoresistive pressure sensor and a surface micromachined silicon on insulator (SOI) pressure sensors are presented, simulated and compared with

respect to output voltage and deflection. The aim of this work is to model, compare and analyze the different performance parameters like deflection, voltage output and sensitivity of different types of sensors and the analysis shows that the double diaphragm SOI sensors show the maximum sensitivity. Finite element tool coventorware ® is used for the simulation.

**II. DESIGN CRITERIA OF PRESSURE SENSORS**

A square diaphragm of sidelength 600µm having thickness 20 µm are designed so that pressure applied per unit area is constant. The substrate is n-type silicon. Anisotropic backside wet etching is performed on the substrate and resulted in a diaphragm of thickness 20 µm. As a general rule the deflection of the diaphragm at the centre must be not greater than the diaphragm thickness and for linear pressure sensing, the deflection should be limited to 1/10<sup>th</sup> of diaphragm thickness . Compared to single silicon sensor , the SOI sensor shows better sensitivity. The SOI wafer has been realized with surface micromachining technique whereas the silicon diaphragm with bulk micromachining. The diaphragm in the conventional sensor is realized by bulk micromachining and the vertical and horizontal edges of the diaphragm are essentially integral part of the substrate. In contrast to this, the diaphragm in the SOI pressure sensor is realized by surface micromachining and the vertical and horizontal edges of the diaphragm are not integral part of the substrate.

In order to increase the pressure range and linearity, a new designing of diaphragm having two diaphragms in a single chip is simulated. An inner diaphragm which works at low pressure and an outer diaphragm surrounding the inner diaphragm works at higher pressures. Fig.2 shows the schematic of single and double diaphragms pressure sensors. In this study, the total diaphragm layer thickness is kept constant. The deflection is simulated and compared for single Si and double silicon and pressure sensor diaphragms for an applied pressure of 0.9 MPa and at different surface concentration (N) ranging from 10<sup>15</sup>cm<sup>-3</sup> to 10<sup>20</sup> cm<sup>-3</sup>. The design parameters of the pressure sensor include membrane size/shape, piezoresistor arrangement, burst pressure and the surface concentration of piezoresistive material.

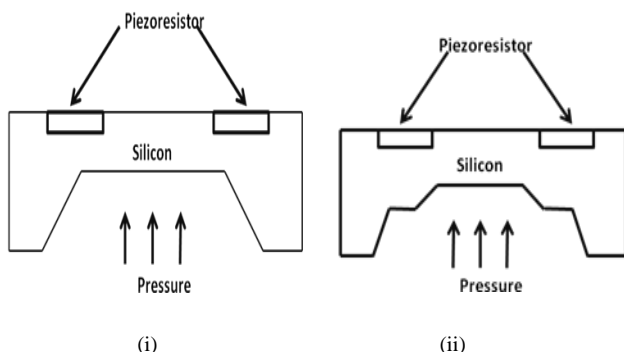


**Fig.2 Different Pressure sensors (i) single diaphragm (ii) Double diaphragm**

The piezoresistors are arranged in a Wheatstone bridge configuration. The bridge is balanced when no pressure is applied on the diaphragm. The application of pressure induces stresses in the diaphragm which causes a change in the resistance of piezoresistors. As a result, the Wheatstone bridge will not be in balance anymore and an output voltage can be measured. The applied pressure on the diaphragm is

limited in such a way that the maximum deflection is limited to 30% of the diaphragm thickness. The maximum deflection of the diaphragm is given by eqn (2).

$$W_{max} = \frac{-0.0138Pa^4}{Eh^3} \tag{2}$$

Where,  $W_{max}$  is maximum deflection, P is applied pressure, a is the length of the diaphragm, E is young’s modulus and h is diaphragm thickness. The maximum stress that a silicon diaphragm can withstand is 7 GPa, which is equal to its fracture stress. Under normal operating conditions stress should never exceed the fracture stress of silicon. The minimum thickness of silicon which gives the maximum sensitivity without damaging the diaphragm is given by eqn (3),

$$h_{min} = \left( \frac{0.39P_B}{\sigma_{max}} \right)^{1/2} \tag{3}$$

Where,  $h_{min}$  is minimum thickness of diaphragm,  $\sigma_{max}$  is maximum stress of silicon diaphragm and  $P_B$  is the burst pressure. Burst pressure is the maximum nondestructive pressure that can be applied to the pressure sensor. It is the pressure at which stress in the diaphragm is equal to the fracture stress. In this analysis burst pressure of 10 MPa is considered and which is 10 times the maximum pressure that is being measured [4].The expression for the maximum stress on the diaphragm can be represented as shown in eqn (4).

$$\sigma_{max} = \frac{0.308Pa^4}{h^2} \tag{4}$$

**III. RESULT AND ANALYSIS**

**A. Deflection Analysis**

The pressure sensors work on the principle of mechanical deformation and stress induced by the application of the measurand pressure. The deformation induces stresses which are then converted into electrical signal output through some means of transduction. The pressure sensors have evacuated cavity which is generated by some means of micromachining on one side of the diaphragm. The deflection and stress analysis of diaphragm having side length 500µm is shown in Fig. 3.

Deflection, stress are observed for a burst pressure of 10 MPa. The maximum pressure applied is 0.9MPa which is less than the one tenth of the burst pressure used for calculating the minimum diaphragm thickness. The maximum stress induced is one tenth of the fracture stress as expected. For getting a linear response one has to consider the condition of deflection and stress so that it always follows a linear relationship.

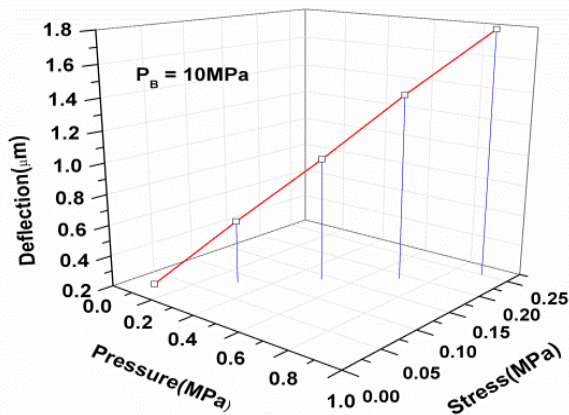


Fig. 3 Deflection and stress analysis of silicon pressure

In a single diaphragm, as the applied pressure increases the nonlinearity increases as the thickness of the diaphragm is fixed. However, in case of a double diaphragm, as the pressure increases, some portion of the pressure is transferred from the inner diaphragm to the outer diaphragm thus increasing the available thickness, sensitivity, linearity and pressure range. A comparison of deflection in the single diaphragm (SD) and double diaphragm is (DD) is shown in Fig.4. For high pressure measurement this method is very much useful so that we will get a wider dynamic range.

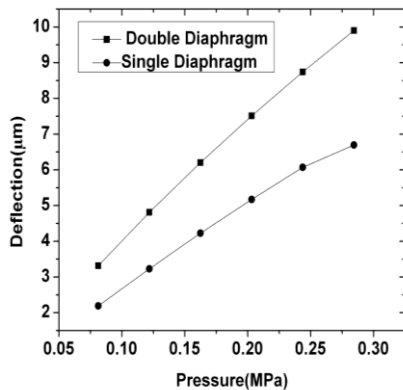


Fig. 4 Comparison of deflection in SD and DD

B. Finite element analysis of silicon and SOI pressure sensors

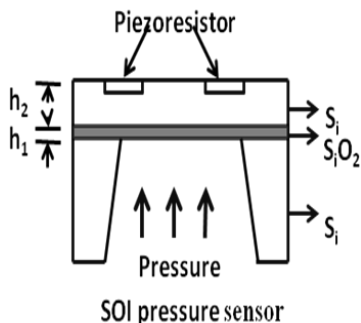


Fig. 5 Deflection and stress analysis of silicon pressure

It is reported that a silicon on insulator pressure sensor give better sensitivity than a silicon pressure sensor [10]. The resistors in the SOI pressure sensor are dielectrically isolated from the diaphragm with the help of the buried oxide layer. This causes a very less leakage current to occur in the sensor

and for which it can be made suitable wider range applications whereas in the Si pressure sensor, the pn junction's isolation allows for more current leakage. This accounts for higher voltage output in SOI Pressure sensor. The difference is attributed to the composite structure of the SOI diaphragm and is shown in Fig.5 where  $h_1$  is the thickness of the buried oxide and  $h_2$  is the thickness of silicon layer. The flexural rigidity of the SOI composite diaphragm is shown in eqn (5) [10]

$$D_{SOI} = \left[ \frac{E_1}{3(1-\nu_1^2)} \left[ (h_1 - h_n)^3 + h_n^3 \right] - \frac{E_2}{3(1-\nu_2^2)} \left[ (h - h_n)^3 + (h_1 - h_n)^3 \right] \right] \quad (5)$$

Where the distance of the center of gravity from the base of composite diaphragms is shown in eqn (6) as

$$h_n = \left[ \frac{(E_1 h_1 Y_1) + (E_2 h_2 Y_2)}{(E_1 h_1) + (E_2 h_2)} \right] \quad (6)$$

$E_1$  and  $E_2$  are the Young's Moduli of the buried oxide and silicon layers of the composite SOI diaphragm respectively. Similarly the Poisson's ratios of these layers are denoted by  $\nu_1$  and  $\nu_2$  where  $Y_1$  and  $Y_2$  are shown in eqn(7)

$$Y_1 = \frac{h_1}{2} \text{ and } Y_2 = h_1 + \frac{h_2}{2} \quad (7)$$

The small scale deflection at the center of the composite SOI diaphragm is obtained as in eqn (8)

$$y_{SOI} = \frac{Pa^4}{4.2 \times 12} \left[ \frac{E_1}{3(1-\nu_1^2)} \left[ (h_1 - h_n)^3 + h_n^3 \right] - \frac{E_2}{3(1-\nu_2^2)} \left[ (h - h_n)^3 - (h_1 - h_n)^3 \right] \right] \quad (8)$$

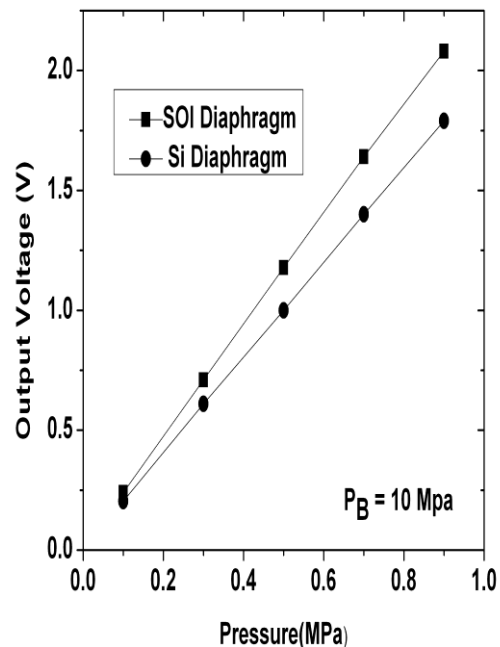
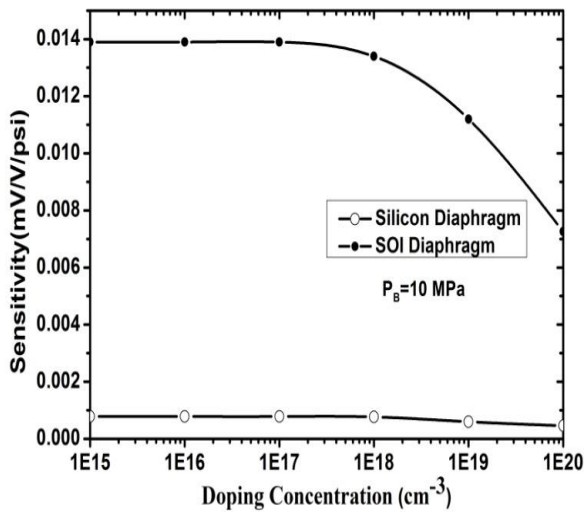


Fig. 6 Voltage output when silicon and SOI are used as pressure sensor diaphragms.

Fig. 6 shows the comparison of silicon and SOI diaphragm with respect to the output voltage and because of the reasons mentioned above, the SOI diaphragm is showing more  $V_{out}$ .



**Fig. 7 Sensitivity with respect to doping concentration in Si and SOI sensors.**

The resistors in SOI pressure sensor offers higher impedance since the piezoresistors are isolated from the substrate by an insulating layer in contrast to the bulk Si pressure sensor where leakage current exist and the impedance of the resistors is less. This accounts for higher voltage output in SOI Pressure sensor. The difference is attributed to the composite structure of the SOI diaphragm. Fig. 7 shows the sensitivity response of silicon and SOI diaphragm.

### C. Sensitivity analysis of different pressure sensors

P-type piezoresistor oriented in the  $\langle 110 \rangle$  direction on a (100) diaphragm plane, which is connected in Wheatstone bridge configuration and it is used as a sensing element. The piezoresistor can be treated as a point at the middle of the diaphragm sides, so the bending moment per unit length acting on the edges parallel to the x axis and y axis are  $M_x$  and  $M_y$  and are given by eqn (9) and eqn (10)[11]

$$M_x = -D \left( \frac{\partial^2 w}{\partial x^2} + \nu \frac{\partial^2 w}{\partial y^2} \right) \quad (9)$$

$$M_y = -D \left( \frac{\partial^2 w}{\partial y^2} + \nu \frac{\partial^2 w}{\partial x^2} \right) \quad (10)$$

$$D = \frac{Eh^3}{12(1-\nu^2)} \quad (11)$$

$$M_x = -0.0513\nu PL^2 \quad (12)$$

$$M_y = -0.0513\nu PL^2 \quad (13)$$

The stress can be calculated by eqn (14) and eqn (15),

$$\sigma_x = \sigma_l = -6 \frac{M_x}{h^2} \quad (14)$$

$$\sigma_y = \sigma_t = -6 \frac{M_y}{h^2} \quad (15)$$

$\sigma_l$  and  $\sigma_t$  are the transverse and longitudinal stress respectively. The fractional change in resistance of a resistor is subjected to longitudinal and transverse stress is given by eqn (16)

$$\frac{\Delta R}{R} = \Pi_l \sigma_l + \Pi_t \sigma_t \quad (16)$$

$$\Pi_{l110} = \frac{1}{2} (\Pi_{11} + \Pi_{12} + \Pi_{44}) \quad (17)$$

$$\Pi_{t110} = \frac{1}{2} (\Pi_{11} + \Pi_{12} - \Pi_{44}) \quad (18)$$

Compared with  $\Pi_{11}, \Pi_{12}, \Pi_{44}$  value dominates in P type materials. Then eqn (17) and eqn (18) can be reduced as,

$$\Pi_{l110} = \frac{1}{2} \Pi_{44} \quad (19)$$

$$\Pi_{t110} = \frac{1}{2} \Pi_{44} \quad (20)$$

The stress on the longitudinal resistor and transverse resistor are equal but act in  $90^\circ$  to each other. The total change in longitudinal and transverse resistance is expressed by eqn (21) and eqn (22) as

$$\frac{\Delta R}{R} = \Pi_{44} (\sigma_l - \sigma_t) \quad (21)$$

$$\text{Thus } \left( \frac{\Delta R}{R} \right)_l = - \left( \frac{\Delta R}{R} \right)_t \quad (22)$$

The general expression for fractional change in p type piezoresistance oriented in  $\langle 110 \rangle$  direction on (100) diaphragm is given by eqn (23),

$$\frac{\Delta R}{R} = \Pi_{44} (\sigma_l - \sigma_t) \quad (23)$$

The resistance change due to the pressure induced stress are expressed as in eqn (24) [12],

$$\frac{\Delta R}{R} = -0.1539 \Pi_{44} \frac{PL^2}{h^2} \quad (24)$$

Where  $\Delta R$  and  $R$  are the change in resistances and resistances respectively. The p-type doping concentration of the piezoresistor is varied from  $10^{15} \text{ cm}^{-3}$  to  $10^{20} \text{ cm}^{-3}$  and doped with boron to make it p-type. The fractional change of resistance due to stress is less and almost constant for higher surface concentration values. For surface concentrations below  $10^{18} \text{ cm}^{-3}$ , the average resistivity of the diffused layer becomes too large for sufficient isolation from the bulk for reasonable layer thickness. However for surface concentrations below  $10^{18} \text{ cm}^{-3}$ ,  $\Pi_{44}$  will reach its limiting values. Fig 8 shows the change in resistance due to stress in piezo resistance for different surface concentration.

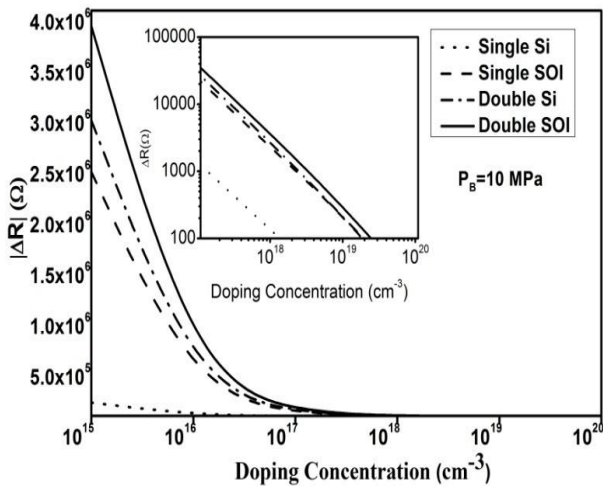


**Fig. 8 Resistance change due to induced stress for different surface concentration (in set change in resistance on log scale)**

A better sensor design requires two important performance factors, namely high output voltage at a given burst pressure and high sensitivity. It is difficult to design a sensor with both the parameters maximized simultaneously, which translates into performance trade-offs. If a sensor exhibits higher sensitivity, it typically offers low burst pressure, as the pressure sensitivity is inversely proportional to burst pressure. Output voltage of a sensor is expressed as in eqn (25)

$$V_{out} = \left( \frac{\Delta R}{R} \right) V_{in} \quad (25)$$

Sensitivity can be expressed in eqn (26)

$$S = \frac{V_{out}}{V_{in}P} \text{ mV/V/Pa} \quad (26)$$

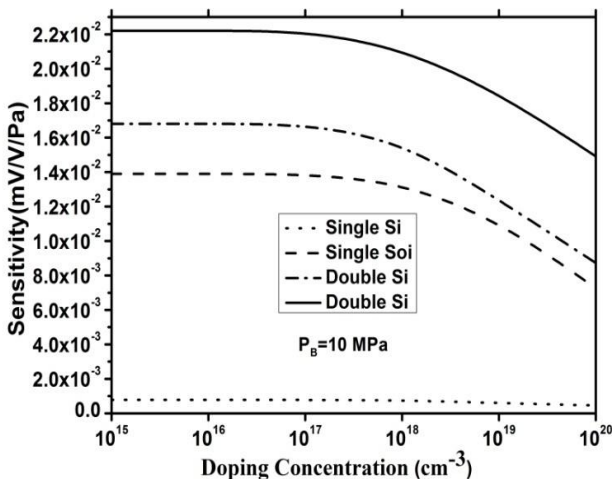


**Fig.9 Variation of sensitivity for different doping concentration**

For evaluating the performance of the pressure sensor the variation of doping concentration of piezoresistor is first considered. At an applied pressure of 10 MPa, the output sensitivity of silicon diaphragm and SOI diaphragm are simulated. The sensitivity of pressure sensor as a function of doping concentration for various diaphragms are shown in Fig.9. Output voltage and sensitivity are constant for surface concentration ranges from  $10^{15} \text{ cm}^{-3}$  to  $10^{17} \text{ cm}^{-3}$ , and

decreases after certain doping concentration, which is about  $10^{17} \text{ cm}^{-3}$  and till the value it remains fairly constant. The pressure is limited to the three times as case of single square diaphragm because of the fact that the linearity of the device should be maintained. At higher pressures, the outer diaphragm will give more output compared with single diaphragm hence increased sensitivity and increased pressure range can be observed by this design. As shown in the Fig.9, double diaphragm SOI shows higher sensitivity when compared with other pressure sensors. When pressure increases, deflection of double diaphragm SOI increases linearly. The results shows that SOI deflects more than the silicon pressure sensor. The difference is attributed to the composite structure of the SOI diaphragm. In SOI diaphragm, the silicon dioxide being amorphous material, the stress developed will be less. The diaphragm in the conventional sensor is realized by bulk micromachining and the vertical and horizontal edges of the diaphragm are essentially integral part of the substrate. In contrast to this, the diaphragm in the SOI pressure sensor is realized by surface micromachining and the vertical and horizontal edges of the diaphragm are not integral part of the substrate. Also the presence of  $\text{SiO}_2$  increases the rigidity of the structure. Hence the deflection of the conventional sensor is more, than in SOI Pressure sensors. Table 1 shows the list of design parameters used throughout the entire simulation.

**Table I List of sensor design parameters**

Parameters	Specifications	
	S	D
Die thickness	385 $\mu\text{m}$	370 $\mu\text{m}$
Diaphragm size	600 $\times$ 600 $\mu\text{m}^2$	Inner 600 $\times$ 600 $\mu\text{m}^2$ Outer 1200 $\times$ 1200 $\mu\text{m}^2$
Doping concentration	$10^{17} \text{ cm}^{-3}$	$10^{17} \text{ cm}^{-3}$
Diaphragm thicknesses	15	30

#### D. Mobility Analysis

The Arora mobility model is used to simulate the doping dependent mobility in Si and it takes into account the scattering of the carriers by charged impurity ions which leads to a degradation of the carrier mobility (ionized impurity scattering) [13]. This model presents a single empirical relationship for carrier mobility as a function of temperature and concentration which can be used for temperature from 77K to 500 K. Arora model gives an empirical relation between temperature and mobility. The hole mobility in a bulk semiconductor ( $\mu_p$ ) is a function of doping concentration N and temperature T which is given by eqn (27).

$$\mu_p = 5.43T_N^{-0.57} + \frac{1.36 \times 10^8 T^{-2.23}}{1 + \left[ \left( \frac{N}{2.35 \times 10^{17} T_N^{2.4}} \right) \right]} 0.88T_N^{-0.146} \quad (27)$$

Where

$$T_N = \frac{T}{300} \quad (28)$$

In general, lattice scattering and ionized impurity scattering are the two scattering mechanisms affecting the hole mobility and here the ionized impurity scattering dominates. So when temperature increases mobility decreases. In this analysis it is assumed that ionization is 100%.

In order to understand the effect of temperature on output voltage the conductivity of the piezoresistor is considered. The conductivity is given by eqn (29) [14]

$$\sigma = q(p\mu_p + n\mu_n) \quad (29)$$

As the material is p-type, minority carrier concentration can be neglected. Then the conductivity is given by eqn (30).

$$\sigma = \frac{1}{qp\mu_p} \quad (30)$$

Resistivity can be expressed as in eqn(31)

$$R = \frac{\rho l}{A} = \frac{1}{qp\mu_p} \frac{l}{A} \quad (31)$$

The conductivity is a function of carrier concentration and mobility. Fig 10 shows the change in carrier mobility in the temperature range from 150K to 450K. When the temperature increases,  $\mu_p$  decreases. Mobility is the crucial parameter to describe the resistance of a bulk material. The mobility is expected to decrease with increasing temperature.

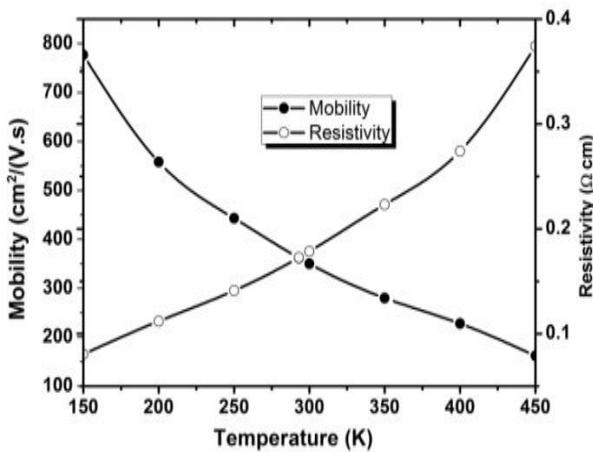


Fig. 10 The mobility and resistivity in boron-doped silicon as a function of various temperature ranges.

#### IV. CONCLUSION

A conventional silicon MEMS pressure sensor and a SOI pressure sensor diaphragm were modeled. Optimizing the doping concentration of piezoresistor as  $10^{17} \text{cm}^{-3}$ , the double SOI shows better pressure sensitivity. The results shows that the silicon pressure sensor exhibited lower deflection and more stresses at its edges, than the SOI pressure sensors. When connected in Wheatstone bridge configuration, the MEMS pressure sensor with SOI diaphragm provides higher voltage output and sensitivity when compared to its silicon counterpart. SOI pressure sensor also provides wider range and better sensitivity. Hence SOI based double diaphragm based MEMS pressure sensors can be used for high pressure applications with better sensitivity when compared to its silicon counterparts.

#### REFERENCES

1. M. X. Zhouet. Al, "A Novel Capacitive Pressure Sensor Based on Sandwich Structures", Journal of microelectro mechanical system, Vol. 14, pp.1272-1282,2005.
2. Bernd Folkmer, Peter Steiner, Walter Lang, A pressure Sensor Based on a nitride membrane using single - crystalline piezoresistors, Sensors and Actuators A 54 (1996) 488-492.
3. A. Berns, U. Buder, E. Obermeier, A. Wolter, A. Leder, Aero MEMS sensor array for high-resolution wall Pressure measurements, Sensors and Actuators A 132 (2006) 104-111.
4. Ingelin Clausen, Ola Sveen, Die separation and packaging of a Surface micromachined piezoresistive pressure sensor, Sensors and Actuators A 133 (2007) 457-466.
5. A.Wisitorsaat, V.Pathanasetakul, T. Lomas, A. Tuantranont, Low cost thin film based piezoresistive MEMS tactile sensor, Sensors and Actuators A 139 (2007) 17-22.
6. Shyam Aravamudhan, Shekhar Bhansali, Reinforced Piezoresistive pressure sensor for ocean depth measurements, Sensors and actuators A 142 (2008) 111-117.
7. K.Sivakumar, N. Dasgupta, K.N. Bhat, Sensitivity enhancement of polysilicon piezo-resistive pressure sensors with phosphorous diffused resistors, Journal of Physics :Conference Series 34 (2006) 216-221
8. KY Madhavi, Sumithradevi K.A, M.Krishna, M.N. Vijayalakshmi, " Analysis of square and circular diaphragms for a MEMS pressure sensor using Data Mining Tool" 2011 International conference on Communication System and Network Technologies
9. Suja K J, Bhanu Pratap Chaudhary, Rama Komaragiri, "Design and simulation of Pressure sensor for Ocean Depth Measurement" ,Applied Mechanics and Materials Vols.313- 314 (2013) pp 666-670
10. Narayanaswamy M ., Joseph Daniel R Sumangala K Antony Jeyasehar C. (2011) Computer aided modelling and diaphragm design approach for high sensitivity silicon-on-insulator pressure 44 : 1924-1936
11. Timoshenko S and Woinosky-Krieger, "Theory of plates and shells "(1987)
12. Shih-Chin Gong and Chengkuo Lee, " Analytical; solution of Sensitivity for pressure microsensors", IEEE Sensors journal Vol 1 , No 14,Dec2004
13. N.D. Arora, J.R. Hauser, D.J. Roulston, "Electron and hole mobilities in silicon as a function of concentration and temperature" IEEE Trans. Electron Devices, vol 29,1982
14. Donald A Neamen, "Semiconductor physics and devices," Tata McGraw-Hill 2007.

#### AUTHORS PROFILE



**Suja K J** has obtained her M Tech Degree in Optoelectronics from Kerala University and is currently working as Assistant professor at NIT Calicut. Her main area of interest involves Simulation and modeling of MEMS devices and VLSI.



**Mrs. Vidya Gopal T V** has obtained her M Tech degree in VLSI from National Institute of technology, Calicut, Kerala, India and is currently working as Assistant Professor at Mar A Thanasius College of Engineering, Kothamangalam Kerala. Her main areas of interest are VLSI and MEMS



**Rama Komaragiri** has acquired his Ph.D. from Technical University of Darmstadt, Germany and his M.Tech in solid state Technology from Indian Institute of Technology, Madras. His main area of interest are Nanoelectronics, Novel Semiconductor Devices, VLSI Power Semiconductor Devices, MEMS, NEMS, Molecular Electronics, Modeling and simulation of Semiconductor Devices. He is currently working as

Associate Professor in the ECE Department in NIT Calicut, Kerala